

Quantifying free tropospheric moisture sources over the western tropical Atlantic with numerical water tracers and isotopes

Svetlana Botsyun¹  | Franziska Aemisegger²  | Leonie Villiger²  |
Ingo Kirchner¹  | Stephan Pfahl¹ 

¹Institute of Meteorology, Freie Universität Berlin, Berlin, Germany

²Institute for Atmospheric and Climate Science, ETH Zurich, Zurich, Switzerland

Correspondence

Svetlana Botsyun, Institute of Meteorology, Freie Universität Berlin, Berlin, Germany.
Email: svetlana.botsyun@fu-berlin.de

Funding information

German Research Foundation (Deutsche Forschungsgemeinschaft, DFG), Grant/Award Number: 441025101; Swiss National Science Foundation, Heavy Cumuli grant, Grant/Award Number: 188731; Deutsches Klimarechenzentrum (DKRZ), Grant/Award Number: bb1247

Abstract

Tropical free-tropospheric humidity plays a crucial role for the Earth's radiative balance and climate sensitivity. In addition to atmospheric humidity, stable water isotopes can provide important information about the hydrological cycle. We use the isotope- and water tagging-enabled version of the COSMO_{iso} model to determine isotopic fingerprints of diagnosed moisture pathways over the western tropical Atlantic (WTA). A convection-permitting, high-resolution (5 km) nudged simulation is performed for January–February 2020. During this period, the target region is characterized by alternating large-scale circulation regimes with different humidity and isotope signatures. Moist conditions in the middle troposphere (300–650 hPa) are associated with moisture transport from the south, east, southeast, as well as evaporation from the North Atlantic, while dry conditions correspond to extratropical transport from the north and west. To predict the contribution of different moisture sources, we used a statistical model based on the local specific humidity and temperature as predictors and obtained an R -squared (R^2) of 0.52. Adding water isotopes improved the prediction ($R^2 = 0.73$), showing that isotopes provide unique information on moisture sources and transport patterns beyond conventional local observations.

KEYWORDS

atmospheric humidity, moisture sources, moisture transport, regional and mesoscale modelling, stable water isotopes, trade wind region free troposphere, water tagging, western tropical Atlantic

1 | INTRODUCTION

Free-tropospheric humidity and low-level clouds over the tropical oceans fundamentally impact on the global radiative balance via the greenhouse effect (Held & Soden,

2000) and by influencing Earth's albedo (Bony & Dufresne, 2005). However, the free-tropospheric moisture content is controlled by the interplay of various processes at different scales, such as long-range moisture transport from various evaporation sources, cloud formation

This is an open access article under the terms of the [Creative Commons Attribution](https://creativecommons.org/licenses/by/4.0/) License, which permits use, distribution and reproduction in any medium, provided the original work is properly cited.

© 2024 The Author(s). *Atmospheric Science Letters* published by John Wiley & Sons Ltd on behalf of the Royal Meteorological Society.

underway, as well as turbulent and convective mixing in the lower-troposphere. Determining the respective effects of these processes is challenging based on conventional observational and modelling techniques only. Furthermore, a correct representation of these moisture cycling processes in climate models and their validation for present-day climate is crucial for future climate projections (Bony et al., 2015; Sherwood et al., 2010; Sherwood et al., 2014) and paleoclimate studies (Boateng et al., 2023; Botsyun et al., 2020; Botsyun et al., 2022).

As moisture transport and mixing processes are difficult to assess from conventional observations, alternative sources of information are required. Stable water isotopologues (H_2^{18}O and HD^{16}O ; hereafter simply denoted as stable water isotopes and expressed in usual δ notation (δD and $\delta^{18}\text{O}$) with respect to Vienna Standard Mean Ocean Water (V-SMOW)) are natural tracers of moist processes in the atmosphere. Stable water isotopes are sensitive to above mentioned important physical processes an air mass undergoes (Galewsky et al., 2005; Galewsky et al., 2016; Gat, 1996), including large-scale transport, detrainment of condensate from convective clouds and its subsequent evaporation (Bony et al., 2008; Risi et al., 2008; Sun & Lindzen, 1993), and vertical mixing associated with convection (Bailey et al., 2013; Dahinden et al., 2021; Kurita, 2013; Villiger & Aemisegger, 2024; Yang & Pierrehumbert, 1994).

The western tropical Atlantic (WTA) during winter is a typical example of a trade wind region. Due to its significance for climate projections, it has been extensively studied in recent years, particularly using observations from the EUREC⁴A field campaign (“Elucidating the Role of Clouds-Circulation Coupling in Climate”; Stevens et al., 2021). However, free-tropospheric circulation patterns, transport pathways, and moisture anomalies in this region remain poorly understood, particularly in winter, when very dry airmasses from the mid latitude jet stream region penetrate deeply into the tropical lower and mid-troposphere, thereby modulating free tropospheric relative humidity (Lang et al., 2023), low-cloud patterns (Aemisegger et al., 2021) and the radiation budget (Villiger et al., 2022). This interaction between tropics and extratropics could change with climate warming and modulate the energy balance in radiatively sensitive dry regions. Here we investigate the sources and isotopic composition of free-tropospheric moisture over the WTA near Barbados. The study period covers January–February 2020 and thus corresponds to the time of the EUREC⁴A, which provides additional opportunities for model evaluation with observational data.

Previous studies have shown that the winter atmospheric circulation in the WTA is dominated by four regimes, contributing to both free-tropospheric and cloud

base moisture: (1) a “typical” trade wind situation with easterly winds bringing moist air from the eastern North Atlantic to the Caribbean (Aemisegger et al., 2021), (2) an extratropical flow regime associated with subsidence related to extratropical dry intrusions (Aemisegger et al., 2021), (3) moisture transport from the south (Villiger et al., 2022), and (4) vertical transport associated with local convective circulations (Villiger & Aemisegger, 2024). However, quantitative studies on the relative contributions of these regimes and thus of different moisture sources to the free troposphere over Barbados and their link to stable isotope composition are currently lacking.

Eulerian moisture tagging is a powerful computational technique that provides information on atmospheric moisture transport from a detailed process-based perspective (Risi et al., 2010; Sodemann et al., 2009). In contrast to other (Lagrangian) moisture source diagnostics, tagging, in particular, explicitly includes the effects of convective and turbulent mixing processes on the water budget (Dahinden et al., 2023; Winschall et al., 2014). In this study, we apply the Eulerian moisture tagging capability of the isotope-enabled COSMO_{iso} model (Dahinden et al., 2023) to investigate the relative contributions of moisture from predefined source regions to the Barbados free troposphere.

This study aims to (1) quantify the contribution of moisture sources to the Barbados region in January and February 2020, (2) investigate how this distribution of moisture sources relates to variations in amount and isotopic composition of water vapour in the free troposphere over Barbados, (3) build a statistical model to predict the moisture sources based on local temperature (T), specific humidity (q_v) and isotope values and (4) determine whether water isotopes provide additional quantitative information on moisture sources compared to T and q_v alone.

2 | METHODS

2.1 | Model and experimental design

We apply the isotope-enabled version (COSMO_{iso}; Pfahl et al., 2012) of the non-hydrostatic limited-area atmospheric model COSMO (Steppeler et al., 2003). Details on the isotopic processes in COSMO_{iso} can be found in Pfahl et al. (2012), Dütsch (2016) and Christner et al. (2018). The isotope-enabled version of COSMO has already been used and evaluated in various regions, including the trade wind region (Dahinden et al., 2021; Dahinden et al., 2023; Villiger et al., 2023). Villiger et al. (2023) performed nested simulations for the WTA using COSMO_{iso}

and concluded that the temporal evolution of the simulations agreed well with EUREC⁴A observations (Bailey et al., 2023), underpinning the ability of the model to reproduce the mesoscale to synoptic-scale variability of water vapour isotope fields in the region. In Villiger et al. (2023) special attention is given to the cloud base level, the formation altitude of shallow cumulus clouds, which are rooted in the thermals of the sub-cloud layer. Different mesoscale cloud base features were investigated in detail in this previous study, including clouds and clear-sky dry-warm patches and their isotopic characteristics. However, the sources and transport pathways of free tropospheric air that feeds the boundary layer with dry-depleted air have not been investigated so far.

We performed a COSMO_{isotag} experiment that is identical to the COSMO_{iso,5 km} experiment in Villiger et al. (2023), except for the water tagging capabilities used in our study. The experiment was run with a horizontal resolution of 0.05° with 60 vertical levels and covers the WTA, including the northern part of the South American continent (Figure 1). The initial and lateral boundary conditions were taken from a nested COSMO_{iso} simulation (Villiger et al., 2023; COSMO_{iso,10 km} at hourly time steps). To keep the long simulation close to reality, the simulation was spectrally nudged towards COSMO_{iso,10 km} horizontal winds above 850 hPa. The COSMO_{iso,10 km} experiment was in turn nudged towards a ECHAM6-wiso global simulation, as detailed in Villiger et al. (2023). Note that cloud fraction and liquid water

content were shown to better agree with aircraft observations at higher spatial resolution in Villiger et al. (2023), with the COSMO_{iso,5 km} experiment showing satisfactory results, while still allowing for a reasonable spatial extent of the model domain.

The water tagging capability of COSMO_{isotag} version (Dahinden, 2022; Winschall et al., 2014) allows us to quantify the different moisture contributions from continental and oceanic evaporation sources. The advantage of this technique compared to trajectory-based methods is that it tracks the water rather than the air masses and thus accounts for the effects of phase changes and small-scale mixing. Figure 1 shows the tracer setup and labels used to specify the tracers. Four passive water vapour tracers are used to tag moisture from evaporative source regions within the model domain. Two of them are continental (tag_SWcont, tag_W): South America and Central America, and two are oceanic (tag_tropAtl, tag_NAtl): tropical Atlantic and North Atlantic. Five tracers tag incoming moisture from the lateral boundaries (tag_SWcont, tag_W, tag_SE, tag_E, tag_N), two of which are combined with the surface evaporation tracers. The last tracer tags water vapour contained in the inner domain at the beginning of the simulation (tag_ini, not shown).

The COSMO_{isotag} simulation covers the time period from 6 January to 22 February 2020, which includes the EUREC⁴A campaign. All simulated days, except for the first 3 days needed for tagging spin-up, are included in the analysis.

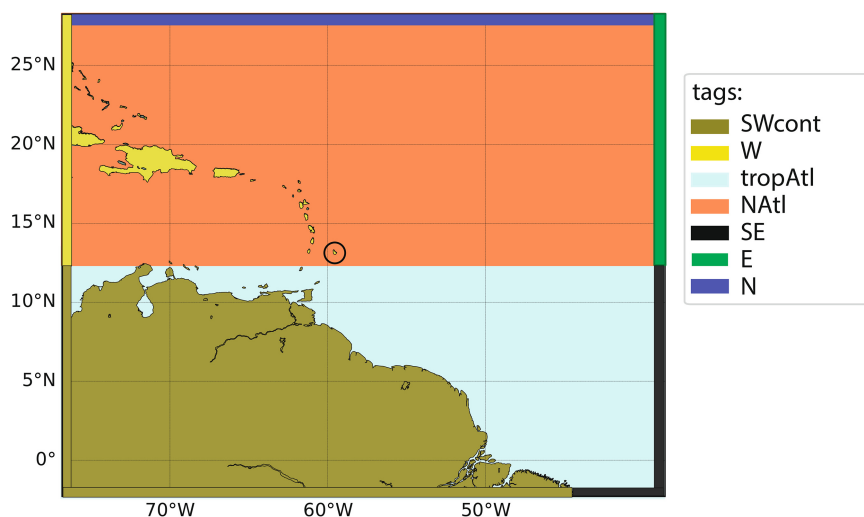


FIGURE 1 Model domain and tracer initialization setup for the COSMO_{isotag} simulation. The land or ocean regions from which the tagged water evaporates are shown by olive green (South America; tag_SWcont), yellow (Central America; tag_W), light blue (tropical Atlantic; tag_tropAtl), and coral (North Atlantic; tag_NAtl) shadings. Atmospheric boxes where water is tagged that flows through are shown in olive green (southern and western boundary; tag_SWcont), yellow (western boundary; tag_W), black (southern and eastern boundary; tag_SE), emerald green (eastern boundary; tag_E), dark blue (northern boundary; tag_N). The moisture that is initially present in the model domain is separately tagged (tag_ini, not shown here). The black circle indicates the island of Barbados.

2.2 | Implementation of the regression model

We have implemented a multiple linear regression model (LR) with polynomial features of cubic degree to predict the target variables (predictands) from the input variables (predictors). LR calculates each predictand as a function of the predictors (see [Supporting Information](#), Equation 1), adjusting the coefficients using the least squares method. Adding polynomial features to the model enables it to capture non-linear relationships between the predictors and the predictands, enhancing its ability to represent complex data patterns. Our goal is to predict the relative contributions of moisture sources to the water content of the middle troposphere over Barbados, using four sets of predictors: (1) q_v and T , (2) q_v , T , and δD , (3) q_v , T , δD ,

$\delta^{18}\text{O}$, and (4) q_v , T , δD , and d-excess and to compare these different sets. The implementation was carried out in the Python programming language using the scikit-learn library, which integrates a number of state-of-the-art machine learning algorithms (Pedregosa, 2011).

For the analysis, we use the time series of the predictors with a frequency of 1 h averaged over 3×3 grid cells over Barbados and between 300 and 650 hPa pressure levels (Figure S1). To prepare the data for model training, we implemented a 10-fold cross-validation procedure. In each iteration, the dataset was randomly split, with 80% of the time steps allocated for training and the remaining 20% reserved for testing. This iterative process was repeated 10 times, each time with a different subset of the data, ensuring that each data point was used in both training and testing phases. The model performance was

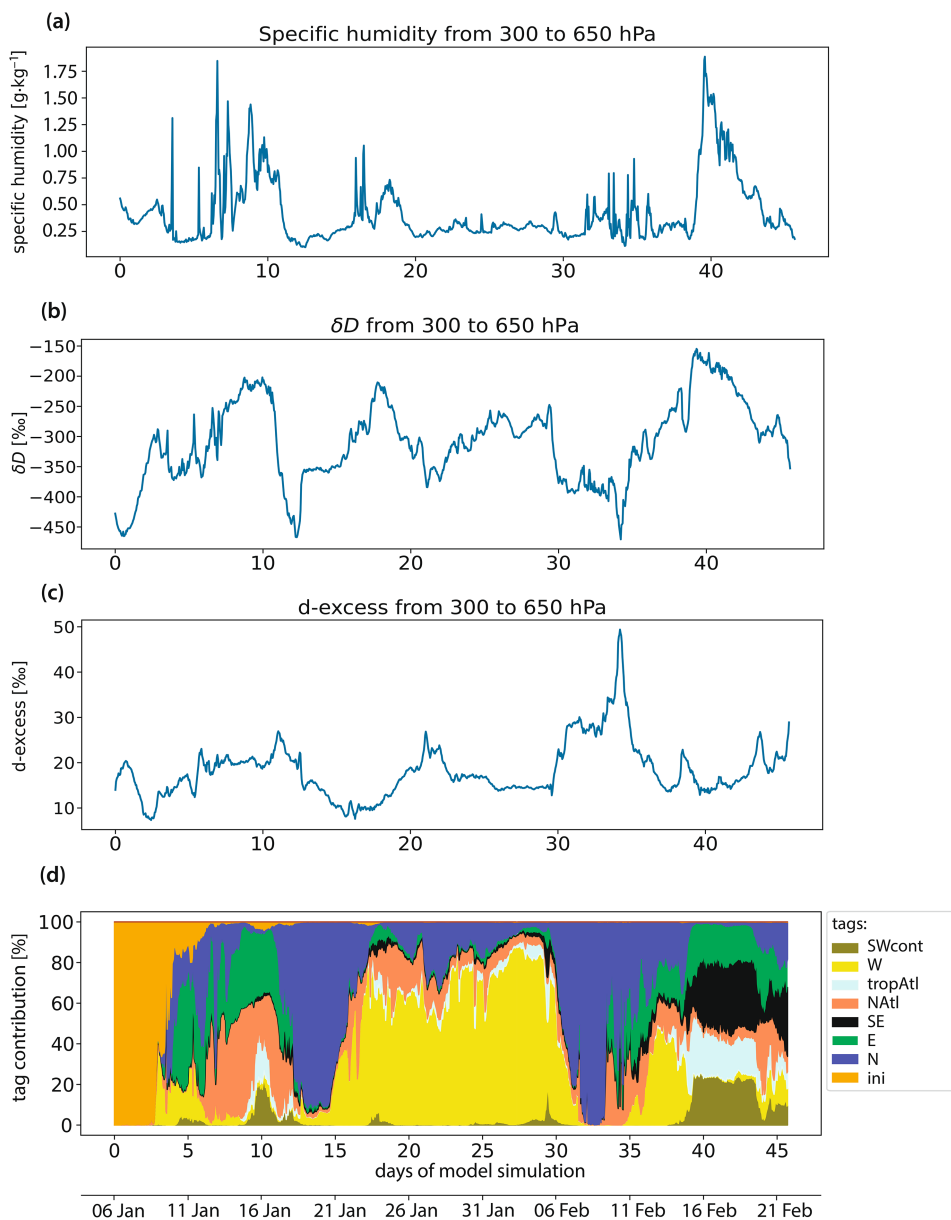


FIGURE 2 COSMO_{iso} model outputs showing time series with 1-h frequency of (a) q_v , (b) δD , (c) d-excess and (d) the fraction of q_v from tracers averaged between 300 and 650 hPa and over 3×3 grid cells over the island of Barbados from January 6 to February 20, 2020. The contribution of initial moisture is below 10% after ~ 72 h of the model run.

evaluated by calculating the root mean square error (RMSE) and the coefficient of determination (R^2) (see [Supporting information](#)).

3 | RESULTS AND DISCUSSION

3.1 | Moisture origin in the free troposphere over Barbados

The specific humidity (q_v) averaged between 300 and 650 hPa over Barbados shows alternating wet and dry conditions: q_v larger than 1 g kg^{-1} prevails from day 6 to day 12 and from day 38 to day 43 (Figure 2a) while all other days are characterized by lower q_v . Short-term q_v variations also occur within these dry and wet periods, but they are mostly smaller than the average differences between the periods.

The moisture sources of this free-tropospheric humidity over Barbados show three alternating regimes (Figure 2d), which correspond to previously detected regional circulation patterns in winter (Aemisegger et al., 2021; Villiger et al., 2023). Regime (i) is associated with moisture transport from the northern domain boundary (Figure 2d, tag_N) and dominates on days 13–15 and 32–33. It is characterized by a contribution of tag_N of up to 90%. Regime (ii) is characterized by moisture transport from the northwestern domain boundary (tag_W contributes more than 60%) and occurs between days 17 and 31. In contrast, regime (iii) is characterized by a mixture of moisture from different source regions

that includes moisture evaporated from the South American continent (tag_SWcont), from the sea surface within the model domain (tag_tropAtl and tag_NAtl), and from the eastern and southern boundaries (tag_E and tag_SE). This regime dominates on days 4–13 and 38–46.

The three regimes also differ in humidity signature (Figures 2a and 3a). Regimes (i) and (ii) are characterized by low humidity, while during regime (iii) high q_v values are simulated in the mid-troposphere over Barbados. However, tag_NAtl and tag_E have both dry and wet signatures. The impact of the three contrasting circulation regimes on the moisture amount above Barbados is reflected in the correlations of q_v with the fraction of q_v from passive tracers (Figure 3b). The Pearson correlation coefficients (r) between q_v and the tag_SEcont and tag_tropAtl tracer fractions are 0.64 and 0.63, respectively, indicating a close relationship between the wet anomalies in the free troposphere over Barbados and moisture transport from evaporation from the South American continent and the tropical Atlantic. Fractions of tag_W and tag_N are significantly negatively correlated with q_v ($r = -0.38$ and $r = -0.44$, respectively), indicating a linkage between extratropical moisture transport and dry conditions over Barbados.

Source regimes (i) and (ii) along with low q_v confirm the importance of large-scale descent from the extratropical upper troposphere for creating dry conditions in the trade wind cloud layer (Villiger et al., 2022). This large-scale circulation pattern is influenced by extratropical Rossby wave breaking over the central North Atlantic with an upper level trough and an intense surface

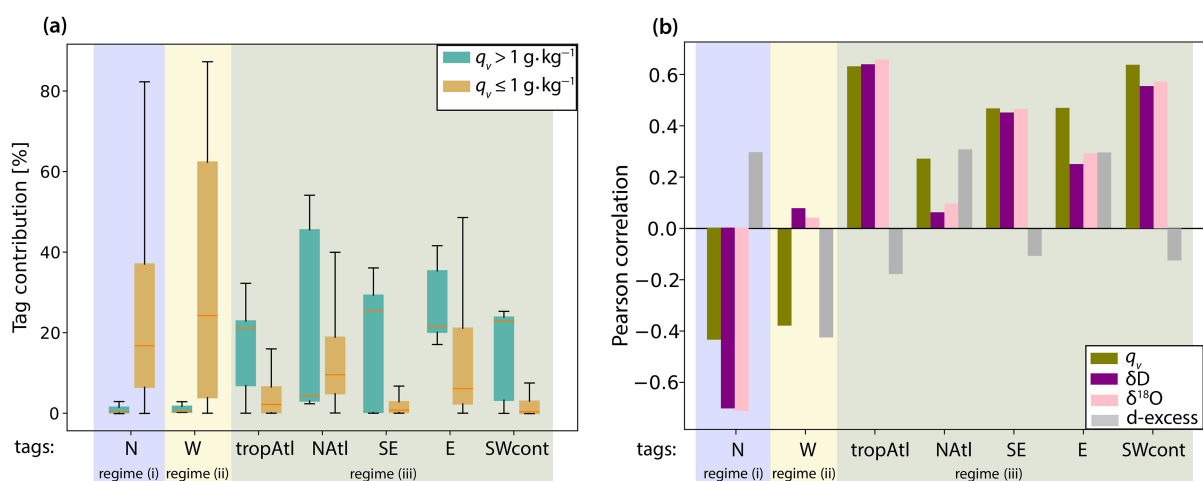


FIGURE 3 (a) Boxplot of the percentage contributions of the moisture sources to the total q_v (tag_SWcont–tag_N) averaged between 300 and 650 hPa over Barbados. The time steps are selected depending on the q_v : the turquoise colour corresponds to the data points with specific humidity greater than 1 g kg^{-1} , the brown colour to the data points with q_v less than 1 g kg^{-1} . The boxes extend from the first quartile to the third quartile of the data, with a red line at the median. The whiskers extend from the box to the farthest data point within 1.5 times the interquartile range of the box. (b) Mean Pearson correlation coefficients between the fraction of q_v from tracers and q_v (olive colour), δD (purple), $\delta^{18}O$ (pink), and d-excess (grey). The values are averaged between 300 and 650 hPa over Barbados.

cyclone underneath (Aemisegger et al., 2021; Villiger et al., 2023). Regarding the wet anomaly on February 14 (day 39 of our simulation), Villiger et al. (2022) linked it to a horizontally extended mixed-phase shelf cloud that persisted for 2 days. The authors show that most precipitation from the shelf cloud evaporated in the underlying dry layer, leading to the formation of downdrafts due to evaporative cooling and thus possibly triggering enhanced shallow convection. Our results partially confirm this, as the free troposphere over Barbados has a relatively high contribution of locally evaporated moisture (tag_tropAtl and tag_NAtl). Meanwhile, the high contribution of tag_SWcont and tag_SE moisture could be related to ascent in the Intertropical Convergence Zone (ITCZ) and detrainment into the trade wind free troposphere.

3.2 | Isotope signals of the different moisture regimes

The three detected contrasting regimes of atmospheric water vapour transport are associated with substantial temporal variability in δD and d-excess (Figure 2b,c). Low δD values ($< -350\text{‰}$) are mainly related to dry conditions, in particular those associated with source regime (i). The Pearson correlation coefficients (r) for the correlation of δD and $\delta^{18}O$ with the tag_N tracer fraction are -0.72 and -0.71 , respectively (Figure 3b). Source regime (iii) is associated with particularly enriched δD values ($> -250\text{‰}$). However, enriched isotopic signatures also appear within the other regimes, in particular in regime (ii). We find a high positive correlation of isotope ratios with the tag_SWcont and tag_tropAtl tracer fractions ($r > 0.55$ for both δD and $\delta^{18}O$), suggesting that enriched isotopic signals are associated with a high relative share of moisture evaporated from the South American continent and the tropical Atlantic. In contrast, tag_W, which is associated with dry conditions in regime (ii), shows a very low correlation with the isotopic composition of both δD and $\delta^{18}O$, but a significant negative correlation with the d-excess values.

To shed more light on the joint moisture and isotope signature of the source regimes, Figure 4 shows scatter plots in the q_v - δD phase space in which the contribution of several tracers is highlighted. Such q_v - δD plots can provide insights into the occurrence of specific processes, such as mixing, Rayleigh distillation, and rain evaporation (Diekmann et al., 2021; Noone, 2012). Transport from the northern extratropics (tag_N) dominates the driest and most depleted part of the diagram, which potentially indicates strong distillation through rainout that the air masses have experienced due to ascent in the extratropics before being transported towards the

Caribbean. This finding is consistent with the conclusions of Aemisegger et al. (2021), who showed that the isotope-depleted conditions over Barbados are related to large-scale subsidence from the extratropics. In addition, some points in the middle of the lower part of the diagram associated with tag_N might point to a contribution of atmospheric moisture recycling (interaction of vapour with rain drops) in this regime (i). Regime (ii) with transport from the west and northwest (tag_W) dominates the middle part of the diagram, with somewhat wetter and less depleted conditions than during regime (i). This signature is more likely characteristic for mixing between drier and wetter air masses. Finally, the most humid data points are dominated by a mixture of sources in regime (iii), as shown exemplarily for tag_SWcont (evaporation from South America) and tag_E (transport from the northeastern boundary with trade winds). Interestingly, tag_E is affected by moisture recycling (points in the middle right part of the diagram), likely due to interaction with drizzle below shallow trade wind clouds. In contrast, there is no such signature in the moisture from South America. This might be related to convective ascent over the continent and transport towards Barbados at middle tropospheric levels in line with the trajectory analysis of Villiger et al. (2022), where rain evaporation is less frequent but ice sublimation can play an important role (de Vries et al., 2022).

3.3 | LR prediction of moisture sources

Having identified the three distinct moisture regimes over Barbados, we test our ability to predict these three states using the LR model described in Section 2.2. We define three sets of predictands, corresponding to relative contribution of: (1) tag_W, (2) tag_N, and (3) tag_SWcont + tag_tropAtl + tag_NAtl + tag_SE + tag_E + tag_ini. The selection of these sets of predictands and the grouping of moisture tags within the sets is defined according to the found moisture regimes, which are explained in more detail in Section 3. The results in Table 1 show that moisture sources are significantly correlated to both thermodynamic and isotopic variables. Based on T and q_v , the LR is able to predict the moisture sources with $R^2 = 0.52$, that is consistent with our finding that the defined moisture regimes have specific moisture signatures. When one isotopic species (δD) is added as a predictor, the prediction improves with $R^2 = 0.66$. The LR is able to predict the moisture sources with $R^2 = 0.73$ when two isotopic species (δD and $\delta^{18}O$), d-excess, T and q_v are used as predictors. This improved skill when adding isotope variables demonstrates and quantifies the additional information on moisture sources and transport pathways contained in isotope data compared to T and q_v alone.

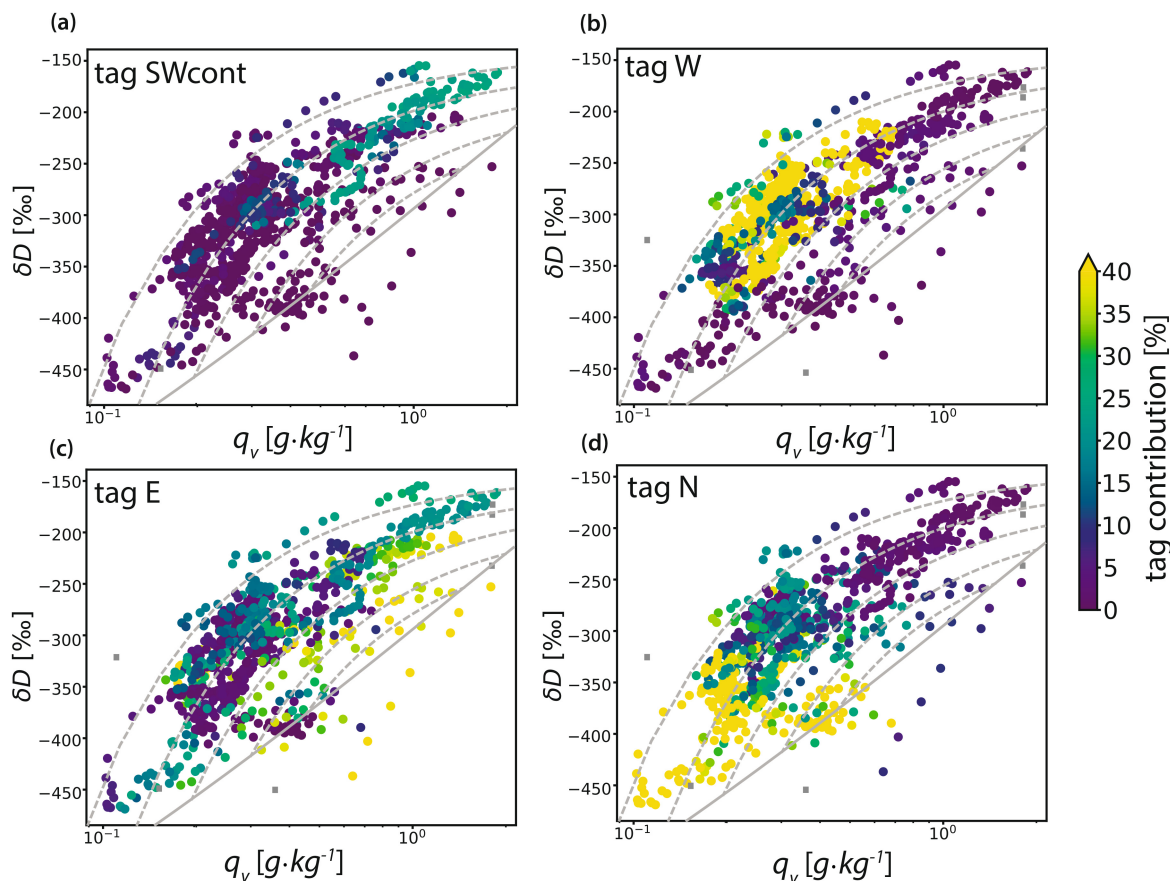


FIGURE 4 Pair distributions of q_v and δD averaged over the mid-troposphere (between 350 and 600 hPa) over Barbados. The colour indicates the relative contributions of specific tags: (a) tag_SWcont, (b) tag_W, (c) tag_E and (d) tag_N. The solid grey line shows the Rayleigh distillation curve for an open system (i.e., assuming 100% precipitation efficiency) for initial conditions of $T_0 = 283^\circ\text{K}$ and $\delta D_0 = -90\text{‰}$. The grey dashed lines show exemplary mixing lines with the mixing end members on the selected Rayleigh distillation curve. Points to the right of the Rayleigh line may indicate moistening by rain evaporation (Worden et al., 2007).

TABLE 1 Root mean square errors (RMSE) and coefficient of determination (R^2) from the multiple linear regression model (LR) for four sets of predictors.

Predictors	RMSE	R^2
q_v, T	20.3	0.52
$q_v, T, \delta D$	17.3	0.67
$q_v, T, \delta D, \delta^{18}\text{O}$	15.4	0.73
$q_v, T, \delta D, \text{d-excess}$	15.9	0.72

Note: Results are shown for the three sets of predictands together. Sets correspond to relative contribution of: (1) tag W, (2) tag N, and (3) tag SWcont + tag tropAtl + tag NATl + tag SE + tag E + tag ini.

4 | CONCLUSIONS

We have simulated the sources of moisture in the free troposphere of the WTA from January to February 2020 using the COSMO_{isotag} model, which incorporates Eulerian water-tagging functionalities, in a convection-

permitting setup. This technique has allowed us to quantify the relative contributions of different moisture source regions to the free troposphere of the target region, taking into account the redistribution of atmospheric moisture through large-scale advection, cloud formation, as well as turbulent and convective mixing. We have confirmed the hypothesis that there are distinct regimes of moisture transport towards the WTA with specific moisture and isotopic signatures over Barbados:

1. Dry periods in the middle troposphere in January–February 2020 are associated with moisture transport from the extratropics, through the northern and the northwestern boundary of our model domain. However, these moisture sources have a different isotopic signature: moisture originating from the north has low δD ($< -350\text{‰}$) and high d-excess values, while moisture transported from the northwest has no distinct signature in δD (small correlation between δD and tag_W) and is linked to relatively low d-excess.

2. Moist periods related to southerly transport from South America and the tropical Atlantic, transport from the trade wind region and local sources. During these periods, the vapour is particularly enriched ($\delta D > -250\text{‰}$).

To test whether moisture sources can be distinguished based on their humidity and isotopic signatures, we formulated a statistical model to predict the origin of moisture based on q_v , T and isotopic parameters (δD , $\delta^{18}\text{O}$ and d-excess) at the selected site. The linear regression model using only q_v , T is able to capture the moisture sources with an R^2 of 0.52. The inclusion of δD as predictor in the regression model improves the prediction of moisture sources with an R^2 of 0.66, while the inclusion of δD together with $\delta^{18}\text{O}$ (or together with d-excess) further improves the prediction of moisture sources with an R^2 of 0.73 (0.72). This result demonstrates the added value of water vapour isotope measurements for a better understanding of the hydrological cycle in tropical regions.

Water tagging is an important tool for deciphering the hydrological cycle but hinges on the atmospheric processes representation, such as convection. The main limitations of this study involve uncertainties in the representation of convection and turbulent transport in COSMO_{isotag}. The good agreement between the modelled and observed q_v and δD values in the middle troposphere over Barbados in January–February 2020 presented in Villiger et al. (2023), who used COSMO_{iso} simulations with the same resolution, indicates a realistic representation of atmospheric processes in the model and gives us confidence to use it in isotope-enabled setup for our study.

While water tagging tracks moisture explicitly, it is computationally expensive. Our regression model offers a more resource-efficient alternative for predicting moisture sources in the region. This model can also be applied to other model simulation results that do not have the capability of water tagging or to observational data. However, testing is needed to validate these applications.

We highlight that the relationships between moisture sources and isotope values over Barbados need further investigation, as our study is limited to two winter months due to the large computational cost of such a high-resolution simulation with many tracers. Longer high-resolution isotope and water tagging simulations, together with continuous measurements, are needed to gain additional insights in the isotopic composition and moisture sources over the WTA and will allow for an investigation of seasonal and inter-annual time scales as well as the relationship between isotope signals and specific weather patterns.

AUTHOR CONTRIBUTIONS

Svetlana Botsyun: Investigation; writing – original draft; methodology; validation; visualization; software; formal analysis; data curation; writing – review and editing; resources; project administration. **Franziska Aemisegger:** Writing – review and editing; validation; methodology; software; data curation. **Leonie Villiger:** Writing – review and editing; validation; methodology; software; data curation. **Ingo Kirchner:** Writing – review and editing; software; validation; resources. **Stephan Pfahl:** Conceptualization; funding acquisition; writing – review and editing; investigation; methodology; validation; supervision; resources; project administration.

ACKNOWLEDGMENT

Open Access funding enabled and organized by Projekt DEAL.

FUNDING INFORMATION

This study was supported by the German Research Foundation (Deutsche Forschungsgemeinschaft, DFG) grant 441025101 (MoWITrade, Modelling water pathways and isotopes in the trade wind boundary layer) to S.P. L. V. was funded by the Heavy Cumuli grant no. 188731 from the Swiss National Science Foundation. This work used computing resources of the Deutsches Klimarechenzentrum (DKRZ) granted by its Scientific Steering Committee (WLA) under project bb1247 and of the HPC Service of FUB-IT, Freie Universität Berlin, Germany.

CONFLICT OF INTEREST STATEMENT

The authors declare no conflicts of interest.

DATA AVAILABILITY STATEMENT

The particular version of the COSMO model used in this study is based on the official version 4.18 with additionally implemented stable water isotope physics and is available under licence (see <http://www.cosmo-model.org/content/consortium/licencing.htm> for more information). The python code of our LR model along with the relevant COSMO output are available from Zenodo repository: <https://zenodo.org/records/12208911>. Complete output of the simulation is available from the authors upon reasonable request.

ORCID

Svetlana Botsyun  <https://orcid.org/0000-0002-5019-0418>

Franziska Aemisegger  <https://orcid.org/0000-0002-4022-9825>

Leonie Villiger  <https://orcid.org/0000-0002-8595-2339>

Ingo Kirchner  <https://orcid.org/0000-0002-4103-6849>

Stephan Pfahl  <https://orcid.org/0000-0002-9872-6090>

REFERENCES

- Aemisegger, F., Vogel, R., Graf, P., Dahinden, F., Villiger, L., Jansen, F. et al. (2021) How Rossby wave breaking modulates the water cycle in the North Atlantic trade wind region. *Weather and Climate Dynamics*, 2(1), 281–309. Available from: <https://doi.org/10.5194/wcd-2-281-2021>
- Bailey, A., Aemisegger, F., Villiger, L., Los, S.A., Reverdin, G., Quiñones Meléndez, E. et al. (2023) Isotopic measurements in water vapor, precipitation, and seawater during EUREC⁴A. *Earth System Science Data*, 15(1), 465–495. Available from: <https://doi.org/10.5194/essd-15-465-2023>
- Bailey, A., Toohey, D. & Noone, D. (2013) Characterizing moisture exchange between the Hawaiian convective boundary layer and free troposphere using stable isotopes in water. *Journal of Geophysical Research: Atmospheres*, 118(15), 8208–8221. Available from: <https://doi.org/10.1002/jgrd.50639>
- Boateng, D., Mutz, S.G., Ballian, A., Meijers, M.J.M., Methner, K., Botsyun, S. et al. (2023) The effects of diachronous surface uplift of the European Alps on regional climate and the oxygen isotopic composition of precipitation. *Earth System Dynamics*, 14(6), 1183–1210. Available from: <https://doi.org/10.5194/esd-14-1183-2023>
- Bony, S. & Dufresne, J. (2005) Marine boundary layer clouds at the heart of tropical cloud feedback uncertainties in climate models. *Geophysical Research Letters*, 32(20), L20806. Available from: <https://doi.org/10.1029/2005GL023851>
- Bony, S., Risi, C. & Vimeux, F. (2008) Influence of convective processes on the isotopic composition ($\delta^{18}\text{O}$ and δD) of precipitation and water vapor in the tropics: 1. Radiative-convective equilibrium and Tropical Ocean-Global Atmosphere-Coupled Ocean-Atmosphere Response Experiment (TOGA-COARE). *Journal of Geophysical Research: Atmospheres*, 113(D19), D19306. Available from: <https://doi.org/10.1029/2008JD009942>
- Bony, S., Stevens, B., Frierson, D.M.W., Jakob, C., Kageyama, M., Pincus, R. et al. (2015) Clouds, circulation and climate sensitivity. *Nature Geoscience*, 8(4), 261–268. Available from: <https://doi.org/10.1038/ngeo2398>
- Botsyun, S., Ehlers, T.A., Koptev, A., Böhme, M., Methner, K., Risi, C. et al. (2022) Middle Miocene climate and stable oxygen isotopes in Europe based on numerical modeling. *Paleoceanography and Paleoclimatology*, 37(10), 1–30. Available from: <https://doi.org/10.1029/2022PA004442>
- Botsyun, S., Ehlers, T.A., Mutz, S.G., Methner, K., Krsnik, E. & Mulch, A. (2020) Opportunities and challenges for paleoaltimetry in “small” orogens: Insights from the European Alps. *Geophysical Research Letters*, 47, e2019GL086046. Available from: <https://doi.org/10.1029/2019GL086046>
- Christner, E., Aemisegger, F., Pfahl, S., Werner, M., Cauquoin, A., Schneider, M. et al. (2018) The climatological impacts of continental surface evaporation, rainout, and subcloud processes on δD of water vapor and precipitation in Europe. *Journal of Geophysical Research: Atmospheres*, 123(8), 4390–4409. Available from: <https://doi.org/10.1002/2017JD027260>
- Dahinden, F. (2022) Tropospheric moisture transport pathways and stable water isotopes over the subtropical North Atlantic. ETH Zurich. Available from: <https://doi.org/10.3929/ethz-b-000537283>
- Dahinden, F., Aemisegger, F., Wernli, H. & Pfahl, S. (2023) Unravelling the transport of moisture into the Saharan Air Layer using passive tracers and isotopes. *Atmospheric Science Letters*, 24(12), e1187. Available from: <https://doi.org/10.1002/asl.1187>
- Dahinden, F., Aemisegger, F., Wernli, H., Schneider, M., Diekmann, C.J., Ertl, B. et al. (2021) Disentangling different moisture transport pathways over the eastern subtropical North Atlantic using multi-platform isotope observations and high-resolution numerical modelling. *Atmospheric Chemistry and Physics*, 21(21), 16319–16347. Available from: <https://doi.org/10.5194/acp-21-16319-2021>
- de Vries, A.J., Aemisegger, F., Pfahl, S. & Wernli, H. (2022) Stable water isotope signals in tropical ice clouds in the West African monsoon simulated with a regional convection-permitting model. *Atmospheric Chemistry and Physics Discussions*, 22, 8863–8895. Available from: <https://doi.org/10.5194/acp-22-8863-2022>
- Diekmann, C.J., Schneider, M., Knippertz, P., de Vries, A.J., Pfahl, S., Aemisegger, F. et al. (2021) A Lagrangian perspective on stable water isotopes during the West African monsoon. *Journal of Geophysical Research: Atmospheres*, 126(19), 1–23. Available from: <https://doi.org/10.1029/2021JD034895>
- Dütsch, M.L. (2016) Stable water isotope fractionation processes in weather systems and their influence on isotopic variability on different time scales. Ph.D. Dissertation 23939, ETH Zurich, Zurich, Switzerland, 159. <https://www.research-collection.ethz.ch/handle/20.500.11850/58>
- Galewsky, J., Sobel, A. & Held, I. (2005) Diagnosis of subtropical humidity dynamics using tracers of last saturation. *Journal of the Atmospheric Sciences*, 62(9), 3353–3367. Available from: <https://doi.org/10.1175/JAS3533.1>
- Galewsky, J., Steen-Larsen, H.C., Field, R.D., Worden, J., Risi, C. & Schneider, M. (2016) Stable isotopes in atmospheric water vapor and applications to the hydrologic cycle. *Reviews of Geophysics*, 54(4), 809–865. Available from: <https://doi.org/10.1002/2015RG000512>
- Gat, J.R. (1996) Oxygen and hydrogen isotopes in the hydrologic cycle. *Annual Review of Earth and Planetary Sciences*, 24(1), 225–262. Available from: <https://doi.org/10.1146/annurev.earth.24.1.225>
- Held, I.M. & Soden, B.J. (2000) Water vapor feedback and global warming. *Annual Review of Energy and the Environment*, 25(1), 441–475. Available from: <https://doi.org/10.1146/annurev.energy.25.1.441>
- Kurita, N. (2013) Water isotopic variability in response to mesoscale convective system over the tropical ocean. *Journal of Geophysical Research: Atmospheres*, 118(18), 10–376. Available from: <https://doi.org/10.1002/jgrd.50754>
- Lang, T., Naumann, A.K., Buehler, S.A., Stevens, B., Schmidt, H. & Aemisegger, F. (2023) Sources of uncertainty in mid-tropospheric tropical humidity in global storm-resolving simulations. *Journal of Advances in Modeling Earth Systems*, 15(6), e2022MS003443. Available from: <https://doi.org/10.1029/2022MS003443>
- Noone, D. (2012) Pairing measurements of the water vapor isotope ratio with humidity to deduce atmospheric moistening and dehydration in the tropical midtroposphere. *Journal of Climate*, 25(13), 4476–4494. Available from: <https://doi.org/10.1029/2011JD015773>
- Pedregosa, F. (2011) Scikit-learn: machine learning in python Fabian. *Journal of Machine Learning Research*, 12, 2825. Available from: <https://github.com/scikit-learn/scikit-learn>
- Pfahl, S., Wernli, H. & Yoshimura, K. (2012) The isotopic composition of precipitation from a winter storm—a case study with the limited-area model COSMO_{iso}. *Atmospheric Chemistry and*

- Physics*, 12(3), 1629–1648. Available from: <https://doi.org/10.5194/acp-12-1629-2012>
- Risi, C., Bony, S. & Vimeux, F. (2008) Influence of convective processes on the isotopic composition ($\delta^{18}\text{O}$ and δD) of precipitation and water vapor in the tropics: 2. Physical interpretation of the amount effect. *Journal of Geophysical Research: Atmospheres*, 113(D19), D19306. Available from: <https://doi.org/10.1029/2008JD009943>
- Risi, C., Bony, S., Vimeux, F., Frankenberg, C., Noone, D. & Worden, J. (2010) Understanding the Sahelian water budget through the isotopic composition of water vapor and precipitation. *Journal of Geophysical Research: Atmospheres*, 115(D24), D24110. Available from: <https://doi.org/10.1029/2010JD014690>
- Sherwood, S.C., Bony, S. & Dufresne, J.-L. (2014) Spread in model climate sensitivity traced to atmospheric convective mixing. *Nature*, 505(7481), 37–42. Available from: <https://doi.org/10.1038/nature12829>
- Sherwood, S.C., Roca, R., Weckwerth, T.M. & Andronova, N.G. (2010) Tropospheric water vapor, convection, and climate. *Reviews of Geophysics*, 48(2), RG2001. Available from: <https://doi.org/10.1029/2009RG000301>
- Sodemann, H., Wernli, H. & Schwiertz, C. (2009) Sources of water vapour contributing to the Elbe flood in August 2002—A tagging study in a mesoscale model. *Quarterly Journal of the Royal Meteorological Society*, 135(638), 205–223. Available from: <https://doi.org/10.1002/qj.374>
- Steppele, J., Doms, G., Schättler, U., Bitzer, H.W., Gassmann, A., Damrath, U. et al. (2003) Meso-gamma scale forecasts using the nonhydrostatic model LM. *Meteorology and Atmospheric Physics*, 82, 75–96. Available from: <https://doi.org/10.1007/s00703-001-0592-9>
- Stevens, B., Bony, S., Farrell, D., Ament, F., Blyth, A., Fairall, C. et al. (2021) EUREC⁴A. *Earth System Science Data*, 13(8), 4067–4119. Available from: <https://doi.org/10.5194/essd-13-4067-2021>
- Sun, D.-Z. & Lindzen, R.S. (1993) Distribution of tropical tropospheric water vapor. *Journal of Atmospheric Sciences*, 50(12), 1643–1660. Available from: [https://doi.org/10.1175/1520-0469\(1993\)050<1643:DOTTWV>2.0.CO;2](https://doi.org/10.1175/1520-0469(1993)050<1643:DOTTWV>2.0.CO;2)
- Villiger, L. & Aemisegger, F. (2024) Water isotopic characterisation of the cloud–circulation coupling in the North Atlantic trades—Part 2: The imprint of the atmospheric circulation at different scales. *Atmospheric Chemistry and Physics*, 24(2), 957–976. Available from: <https://doi.org/10.5194/acp-24-957-2024>
- Villiger, L., Dütsch, M., Bony, S., Lothon, M., Pfahl, S., Wernli, H. et al. (2023) Water isotopic characterisation of the cloud-circulation coupling in the North Atlantic trades. Part 1: a process-oriented evaluation of COSMO iso simulations with EUREC⁴A observations. *Atmospheric Chemistry and Physics*, 23, 14643–14672. Available from: <https://doi.org/10.5194/acp-23-14643-2023>
- Villiger, L., Wernli, H., Boettcher, M., Hagen, M. & Aemisegger, F. (2022) Lagrangian formation pathways of moist anomalies in the trade-wind region during the dry season: two case studies from EUREC⁴A. *Weather and Climate Dynamics*, 3(1), 59–88. Available from: <https://doi.org/10.5194/wcd-3-59-2022>
- Winschall, A., Pfahl, S., Sodemann, H. & Wernli, H. (2014) Comparison of Eulerian and Lagrangian moisture source diagnostics—the flood event in Eastern Europe in May 2010. *Atmospheric Chemistry and Physics*, 14(13), 6605–6619. Available from: <https://doi.org/10.5194/acp-14-6605-2014>
- Worden, J., Noone, D. & Bowman, K. (2007) Importance of rain evaporation and continental convection in the tropical water cycle. *Nature*, 445(7127), 528–532. Available from: <https://doi.org/10.1038/nature05508>
- Yang, H. & Pierrehumbert, R.T. (1994) Production of dry air by isentropic mixing. *Journal of Atmospheric Sciences*, 51(23), 3437–3454. Available from: [https://doi.org/10.1175/1520-0469\(1994\)051<3437:PODABI>2.0.CO;2](https://doi.org/10.1175/1520-0469(1994)051<3437:PODABI>2.0.CO;2)

SUPPORTING INFORMATION

Additional supporting information can be found online in the Supporting Information section at the end of this article.

How to cite this article: Botsyun, S., Aemisegger, F., Villiger, L., Kirchner, I., & Pfahl, S. (2024). Quantifying free tropospheric moisture sources over the western tropical Atlantic with numerical water tracers and isotopes. *Atmospheric Science Letters*, 25(12), e1274. <https://doi.org/10.1002/asl.1274>